Purine Nucleoside Phosphorylase. Catalytic Mechanism and Transition-State Analysis of the Arsenolysis Reaction†

Paul C. Kline and Vern L. Schramm*

Department of Biochemistry, Albert Einstein College of Medicine, Bronx, New York 10461

Received July 19, 1993; Revised Manuscript Received September 23, 1993®

ABSTRACT: Purine nucleoside phosphorylase from calf spleen catalyzes the arsenolysis of inosine to form hypoxanthine and ribose 1-arsenate, which spontaneously hydrolyzes to ribose and arsenate. In the presence of $H_2{}^{18}O$, no ^{18}O is incorporated into ribose, demonstrating that ribose 1-arsenate hydrolysis occurs by attack of water on the arsenic atom. Rapid reaction kinetics at 20 °C result in a biphasic rate curve with the first turnover occurring at a rate of 20 s^{-1} followed by a steady-state rate of 2 s^{-1}. The product burst is consistent with rapid steps for substrate binding and arsenolysis followed by rate-limiting hypoxanthine release at a rate of 2 s^{-1}. Purine nucleoside phosphorylase with bound [^{14}C]inosine was mixed with excess unlabeled inosine and arsenate to determine relative rates for reaction or dissociation of bound inosine. The commitment factor (product formed/inosine released) was 0.19 at saturating arsenate, indicating that inosine binds to free enzyme and that bound inosine is not in thermodynamic equilibrium with free substrate. At neutral pH, kinetic isotope effects for the phosphorolysis reaction are small, indicating kinetic suppression. Kinetic isotope effects for arsenolysis were measured with [1′-^{3}H]-, [2′-^{3}H]-, [1′-^{14}C]-, [9-^{15}N]-, [4′-^{3}H]-, and [5′-^{3}H]inosine to provide experimental values of 1.118 ± 0.003, 1.128 ± 0.003, 1.022 ± 0.005, 1.009 ± 0.004, 1.007 ± 0.003 and 1.028 ± 0.004 respectively. Following correction for commitment factors, the intrinsic isotope effects were matched to a geometric transition-state model selected by bond-energy bond order vibrational analysis. The transition state consistent with all isotope effects has a substantial decrease in the C1′–N9 glycosyl bond order, oxycarbonium character in the ribosyl ring, and weak participation of the arsenate nucleophile. Loss of the C1′–N9 bond is far ahead of the arsenate attack. The X-ray crystal structure for purine nucleoside phosphorylase with bound 9-deazainosine and inorganic sulfate places the nearest oxygen of the sulfate 4.2 Å from C1′ of the nucleoside analogue. This structure is consistent with a mechanism in which the ribosyl group is nearly dissociated from the base prior to attack of the arsenate.

Purine nucleoside phosphorylase (PNP, E.C. 2.4.2.1) catalyzes the reversible phosphorolysis of inosine and guanosine according to the reaction:

purine nucleoside + $PO_4 \rightleftharpoons$ purine base + α-D-ribose 1-phosphate (1)

The reaction is freely reversible, and the equilibrium favors formation of purine nucleosides, although the physiological reaction is phosphorolysis of purine nucleosides (Parks & Agarwal, 1972). A genetic loss of PNP activity causes T-cell immunodeficiency (Giblett et al., 1975; Gelfand et al., 1978; Siegenbeek et al., 1977). The near-specific effect of PNP deficiency on T-cells has generated interest in the development of PNP inhibitors for possible intervention in rheumatoid arthritis, tissue rejection, and chemotherapy for T-cell leukemias (Stoeckler et al., 1986; Kazmers et al., 1981). The crystal structure of the human erythrocyte enzyme has been determined (Ealick et al., 1990), which confirmed the trimeric subunit structure proposed earlier (Edwards et al., 1973).

The kinetic mechanism for PNP has been reported to be ordered with the nucleoside or base binding first (Kim et al., 1968; Krenitsky, 1967). However, a recent study has reported that the calf spleen enzyme binds phosphate prior to the purine nucleoside (Porter, 1992). α-Secondary deuterium kinetic isotope effects for the phosphorolysis of inosine have indicated that the reaction has oxycarbonium character at the transition state, but substantial isotope effects are seen only at pH extremes with the *Escherichia coli* enzyme (Stein & Cordes, 1981; Lehikoinen et al., 1989).

Quantitative analysis of kinetic isotope effects has the potential to provide detailed information on the structure of the transition state for enzymatic reactions (Mentch et al., 1987; Markham et al., 1987; Parkin et al., 1991; Horenstein et al., 1991; Horenstein & Schramm, 1993a). Analysis of kinetic isotope effects is complicated for reversible reactions and for those with intermediates (Northrop, 1981; Cleland, 1987). The arsenolysis reaction catalyzed by PNP is similar to phosphorolysis (eq 1), but the product ribose 1-arsenate is unstable and rapidly hydrolyzes to ribose and arsenate (Parks & Agarwal, 1972). This step renders the reaction irreversible under initial rate assay conditions and simplifies interpretation of kinetic isotope effects:

purine nucleoside + $AsO_4 \xrightarrow{PNP}$ purine base + ribose 1-arsenate $\xrightarrow{H_2O}$ ribose + AsO_4 (2)

The arsenolysis reaction has not been characterized to establish the rate-limiting step(s), the expression of isotope effects, or the kinetic or chemical reaction mechanism. An understanding of the reaction mechanism is necessary for the interpretation of kinetic isotope effects. Once the intrinsic values of the kinetic isotope effects are established, they can be used to provide detailed information of transition-state structure and to provide a blueprint for the design of transition-state inhibitors (Horenstein & Schramm, 1993a,b).

This work describes a mechanistic analysis of the arsenolysis reaction of PNP from bovine spleen using kinetic isotope effects, rapid reaction kinetics, solvent incorporation studies,

† This work was supported by Research Grant GM41916 from the National Institutes of Health.

* Address correspondence to this author at the Department of Biochemistry, Albert Einstein College of Medicine, 1300 Morris Park Ave., Bronx, NY 10461. Tel: (718) 430-2813. FAX: (718) 892-0703.

® Abstract published in *Advance ACS Abstracts,* November 15, 1993.

0006-2960/93/0432-13212$04.00/0

and isotope trapping experiments. The results permit the determination of intrinsic kinetic isotope effects, which are used to describe a geometric model of the enzymatic transition state. These studies are practical only for the arsenolysis reaction since phosphorolysis provided insignificant isotope effects at physiological pH values.

EXPERIMENTAL PROCEDURES

Materials. Adenosine deaminase, alkaline phosphatase, hypoxanthine, and inosine were purchased from Sigma Chemical Co. Labeled glucose was purchased from Amersham, and labeled ribose from American Radiolabeled Chemicals. Sephadex G-25 resin was purchased from Pharmacia Co. $H_2{}^{18}O$ (97 atom %) was purchased from Merck Isotope Co. Purine nucleoside phosphorylase (bovine spleen) in 3.2 M ammonium sulfate was obtained from Sigma Chemical Co. The enzyme was desalted on a gel filtration column of Sephadex G-25 resin (2.5 × 16.5 cm) eluted with 50 mM triethanolamine, pH 7.5, containing 1 mM dithiothreitol. The purity of the enzyme was determined by denaturing polyacrylamide gel electrophoresis. The enzyme was >90% homogeneous and was used without further purification. Enzyme was stored in the desalting buffer and was used within 72 h after desalting.

Labeled Nucleosides. Isotopically labeled AMPs were prepared from labeled riboses, glucoses, and adenine by chemical and enzymatic synthesis according to previously published procedures (Parkin et al., 1984; Parkin & Schramm, 1987). Labeled AMPs were converted to inosine using adenosine deaminase and alkaline phosphatase (Horenstein et al., 1991). Labeled inosines were stored at −70 °C in 50% aqueous ethanol.

Measurement of Kinetic Isotope Effects. Kinetic isotope effects were determined by comparing the relative rates of product formation from labeled and natural-abundance inosines. Reaction mixtures contained a pair of inosines, one labeled with ^3H, and one labeled with ^{14}C, in the ribosyl groups. One radiolabel was located in the isotopically sensitive position (the isotopic substitution), while the other radiolabel was located in the 5′-position, of the ribosyl residue, remote from the reaction center. The [1′-^{14}C]- and [9-^{15}N]inosine kinetic isotope effects used [5′-^{3}H]inosine to report on the reaction rate of the natural-abundance substrate. However, a significant kinetic isotope effect was determined for [5′-^{3}H]inosine; thus it was necessary to correct the 1′-^{14}C and 9-^{15}N kinetic isotope effects by the value of the 5′-^{3}H kinetic isotope effect.

For each kinetic isotope effect experiment, two sets of reactions were analyzed, both using the same substrate mixture. One was allowed to react to 20–30% completion, and the other, to 100% completion. The 100% reaction provided the control ratio of $^3H/^{14}C$, and the 20–30% reaction provided the $^3H/^{14}C$ ratio influenced by the presence of the kinetic isotope effect. The product ribose was resolved from the substrate by chromatography on charcoal, and the $^3H/^{14}C$ ratio was used to calculate the kinetic isotope effect (Parkin & Schramm, 1984). As this is a trace-label technique, the information obtained from these experiments is the V_{max}/K_m kinetic isotope effects.

Calculation of Kinetic Isotope Effects. Kinetic isotope effects were measured by analyzing three or four samples removed from a common reaction mixture containing ^{14}C- and ^3H-labeled substrates. The $^3H/^{14}C$ ratio was determined by scintillation counting of the product ribose following chromatography to resolve ribose from unreacted inosine. The average $^3H/^{14}C$ ratios for partial and complete conversion to products were calculated and expressed as the ratio of the partial to the complete reaction to provide an experimental kinetic isotope effect for each cycle of scintillation counting. A minimum of six cycles of scintillation counter analyses were used to calculate the average kinetic isotope effect for each of the replicate samples.

Transition-State Modeling. The transition-state geometry was modeled using the BEBOVIB-IV program [*Quantum Chemistry Program Exchange*, No. 337; Sims et al. (1977)], which is used to calculate kinetic isotope effects for a preselected transition-state structure. Transition-state structure was varied systematically to match the observed kinetic isotope effects. The acceptable transition state gave a chemically reasonable structure and matched all of the intrinsic kinetic isotope effects. The atomic geometry of reactant-state inosine was derived from the crystal structure (Munns & Tollin, 1970). Hydrogens were added to inosine and positioned by energy minimization using the PM3 semiempirical molecular orbital procedure as implemented in the MOPAC 6.0 system (Stewart, 1989; Merz & Besler, 1990). Force constants for the various vibrational modes were derived from reported values (Sims & Fry, 1974; Sims & Lewis, 1984). The starting structure for the transition state of the ribose ring portion of inosine was derived from the X-ray crystal structure coordinates for ribonolactone (Kinoshita et al., 1981). The initial C–H bond lengths for the transition state were set equal to the values determined for the ribose portion of inosine. Systematic variation in the C1′–N9, C1′–H1′, C1′–04′, C1′–C2′, C2′–H2′ and C1′–arsenate bonds were used to establish the transition state which matched intrinsic isotope effects (Mentch et al., 1987; Horenstein et al., 1991).

Commitment to Catalysis. Isotope trapping experiments were carried out using the pulse-chase method described by Rose (1980). Reaction mixtures (24 μL, total volume) contained 400 μM [8-^{14}C]inosine in 50 mM triethanolamine, pH 7.5, and 30 μM of PNP. The reaction mixture was incubated for 10 s, and a 1-mL chase solution, containing 5 mM inosine and variable concentrations of sodium arsenate from 0.1 to 10 mM in 50 mM triethanolamine, pH 7.5, was added. After 10 s (approximately 20 turnovers) the reaction was terminated by the addition of 100 μL of 1 N HCl. The reaction mixture was concentrated under reduced pressure in a Savant Speed-Vac and analyzed for hypoxanthine and inosine by reverse-phase HPLC using a Waters C_{18} μBondapak column eluted with 5% MeOH in distilled water at 1 mL/min. One-milliliter fractions were collected, 10 mL of scintillation fluid was added, and the fractions were analyzed for radioactivity by liquid scintillation counting.

Control experiments were used to correct for the fraction of total inosine reacted following addition of the chase solution. This fraction was determined by including the labeled inosine in the 1-mL chase solution rather than with the enzyme. The amount of hypoxanthine formed in the control experiment was subtracted from the hypoxanthine formed in the experiment. Formation of the enzyme·inosine complex was necessarily brief since the enzyme catalyzes the slow hydrolysis of inosine (Kline & Schramm, 1992). Times were carefully controlled to prevent hydrolysis prior to addition of arsenate.

Rapid Reaction Kinetics. Rapid reaction kinetics were carried out on a Model RQF-3 quench–flow apparatus purchased from KinTec Instruments of University Park, PA. The reaction components were equilibrated at 20 °C for 10 min before the reaction was initiated. The reaction was initiated by mixing equal volumes of purine nucleoside phosphorylase (40 μM) and sodium arsenate (50 mM) with

Table I: Kinetic Isotope Effects for Phosphorolysis of Inosine by Purine Nucleoside Phosphorylase[a]

substrates	isotope effect	exptl kinetic isotope effect
[1′-^{3}H]inosine + [5′-^{14}C]inosine	1′-^{3}H, α-secondary	1.047 ± 0.002 (6)[b]
[1′-^{14}C]inosine + [5′-^{3}H]inosine	1′-^{14}C, primary	1.000 ± 0.001 (15)
[5′-^{3}H]inosine + [5′-^{14}C]inosine	5′-^{3}H, γ-secondary	1.001 ● 0.003 (6)

[a] Experimental conditions: 1 mM inosine and 200 mM phosphate, pH 7.5. [b] The number of experiments that were averaged to determine the isotope effect is shown in parentheses.

[8-^{14}C]inosine (800 μM). The total reaction volume from both sample loops was 82 μL. The reaction was quenched by the addition of 2 N HCl (68 μL). Reaction times varied from 3 to 900 ms, and the products of the reaction were resolved by chromatography on a Waters C_{18} μBondapak HPLC column eluted with 5% MeOH in water and quantitated by scintillation counting.

The KINSIM kinetic simulation program was used to assign rate constants to the results of the rapid quench experiments (Barshop et al., 1983). Individual rate constants were varied to fit the experimental points while the known dissociation constants for inosine, hypoxanthine, and arsenate were maintained at constant values.

Mechanism of Ribose 1-Arsenate Hydrolysis. To a reaction mixture consisting of 10 mM inosine, 20 mM sodium arsenate, and 5 mM ammonium bicarbonate, pH 7.5, in 90 μL of $H_2{}^{18}O$ (97 atom %) was added 10 μL of PNP (4 μg/μL). After 5 min the reaction mixture was frozen and lyophilized. The half-time of exchange for $As^{18}O_4$ in H_2O has been reported to be 44 min at pH 8.0 and 32 °C (Kouba & Varner, 1959). Analysis of the reaction mixture by reverse-phase HPLC on a C_{18} μBondapak column eluted with 5% MeOH in water indicated that 70% of the inosine had been cleaved.

The product ribose was reduced to the alditol acetate using the method of Blakeney et al. (1983). The freeze-dried reaction mixture was dissolved in 300 μL of dimethyl sulfoxide containing sodium borohydride (20 mg/mL). The mixture was heated to 40 °C for 90 min after which 100 μL of glacial acetic acid was added. 1-Methylimidazole (60 μL) and acetic anhydride (300 μL) were added, and the reaction mixture was incubated for 10 min at room temperature. Water (1.5 mL) was added, and the mixture was extracted with 300 μL of methylene chloride. The bottom organic layer containing the alditol acetate was removed and analyzed by fast atom bombardment mass spectrometry on a Finnigan MAT 90 mass spectrometer.

[1-^{18}O]Ribose was synthesized by heating D-ribose (20 mM) dissolved in $H_2{}^{18}O$ at 100 °C for 5 h (Cortes et al., 1991). After exchange was complete, the $H_2{}^{18}O$ was removed under reduced pressure and the labeled ribose was reduced, acetylated, and analyzed by mass spectrometry as described above. The half-time for exchange of [1-^{18}O]ribose into solvent at pH 5.9 and 25 °C is 24 h. Thus the [1-^{18}O]ribose was stable during experiments which exposed [1-^{18}O]ribose to solvent for 5 min at pH 7.5 and 30 °C.

RESULTS

Kinetic Isotope Effects. Phosphorolysis of inosine in the presence of both low and high phosphate concentrations gave small or negligible kinetic isotope effects (Table I). The lack of substantial isotope effects with either [1′-^{14}C]- or [1′-^{3}H]-inosine was observed at both high and low phosphate concentrations and indicated that commitment factors or internal equilibria prevented expression of isotope effects. Isotope effects near unity cannot be easily corrected since the large correction factors would introduce unacceptable errors in estimating intrinsic isotope effects.

Arsenolysis of inosine gave substantial kinetic isotope effects with most of the labeled inosines (Table II). Dissociative mechanisms (S_N1-like) give large α- and β-secondary isotope effects and modest 1′-^{14}C primary effects, while associative (S_N2-like) mechanisms result in large 1′-^{14}C primary effects and small secondary effects. The arsenolysis reaction agrees with dissociative character at the transition state in which C1′-O4′ acquires oxycarbonium character and C1′ is partially rehybridized to sp^2. The substantial isotope effect for [5′-^{3}H]inosine suggests distortion of the 5′ carbon at the transition state. The observed 9-^{15}N kinetic isotope effect of 1.009 ● 0.004 is smaller than that observed for C–N glycosyl bond cleavage by acid or by nucleoside and nucleotide *N*-glycohydrolases (Parkin & Schramm, 1987; Horenstein et al., 1991). To ensure the accuracy of this value, the same substrate mixture used to determine the 9-^{15}N primary isotope effect in Table II was used with nucleoside hydrolase and was shown to give a 9-^{15}N isotope effect of 1.024 ± 0.003 which agrees well with the previously reported value of 1.026 ± 0.004 (Horenstein et al., 1991). The 1′-^{14}C primary isotope effect was subject to a large correction when 5′-^{3}H was used as the remote label; therefore, the value for the 1′-^{14}C primary isotope effect was verified by using [4′-^{3}H]inosine for the remote label. This required a correction factor of only 1.007 ● 0.003. Primary 1′-^{14}C isotope effects agreed to within experimental error when determined by both methods.

Commitment to Catalysis. The commitment of enzyme-bound inosine to catalysis was determined using the isotope trapping method described by Rose (1980). The amount of inosine converted to hypoxanthine as a function of sodium arsenate concentration present in the chase solution was determined and is summarized in Figure 1. The inosine concentration in the pulse solution was 400 μM or approximately $50K_m$. Under these conditions, the enzyme active sites are 0.98 saturated with inosine. When extrapolated to saturating sodium arsenate concentration, 4.8 μM hypoxanthine was formed with a PNP concentration of 30 μM. For each inosine bound to PNP, 0.16 hypoxanthine was formed. The commitment for bound inosine is defined as the ratio of product formed to substrate released and is 0.19.

Northrop (1981) has derived an expression which relates intrinsic isotope effects to observed isotope effects and commitments to catalysis.

$$^{D}(V/K) = \frac{^{D}k + c_f + c_r{}^{D}K_{eq}}{1 + c_f + c_r} \quad (3)$$

where $^{D}(V/K)$ is the observed isotope effect (deuterium in this example), c_f is the forward commitment to catalysis, c_r is the reverse commitment to catalysis, $^{D}K_{eq}$ is the equilibrium isotope effect, and ^{D}k is the intrinsic isotope effect. The irreversible hydrolysis of ribose 1-arsenate together with the rapid release of ribose 1-arsenate under initial rate conditions (see Discussion) is likely to make the reverse commitment negligible relative to the other terms in eq 3. Under these conditions, the expression reduces to

$$^{D}(V/K) = \frac{^{D}k + c_f}{1 + c_f} \quad (4)$$

The kinetic isotope effects corrected for the forward commitment are listed in Table II.

Table II: Kinetic Isotope Effects for Arsenolysis by Purine Nucleoside Phosphorylase[a]

substrates	isotope effect	exptl kinetic isotope effects[b]	intrinsic kinetic isotope effects[c]
[1′-^{3}H]inosine + [5′-^{14}C]inosine	1′-^{3}H, α-secondary	1.118 ± 0.003 (6)[d]	1.141 ± 0.004
[2′-^{3}H]inosine + [5′-^{14}C]inosine	2′-^{3}H, β-secondary	1.128 ± 0.003 (6)	1.152 ± 0.003
[1′-^{14}C]inosine + [5′-^{3}H]inosine	1′-^{14}C, primary[e]	1.022 ± 0.005 (6)	1.026 ± 0.006
[1′-^{14}C]inosine + [4′-^{3}H]inosine	1′-^{14}C, primary[e]	1.020 ± 0.006 (3)	
[9-^{15}N,5′-^{14}C]inosine + [5′-^{3}H]inosine	9-^{15}N, primary[e]	1.009 ± 0.004 (9)	1.010 ± 0.005
[4′-^{3}H]inosine + [5′-^{14}C]inosine	4′-^{3}H, δ-secondary	1.007 ± 0.003 (3)	1.008 ± 0.004
[5′-^{3}H]inosine + [5′-^{14}C]inosine	5′-^{3}H, γ-secondary	1.028 ± 0.004 (6)	1.033 ± 0.005

[a] Experimental conditions: 800 μM inosine and 50 mM arsenate, pH 7.5. [b] The experimental kinetic isotope effects are corrected for the extent of substrate hydrolysis since the ^{3}H/^{14}C ratio of inosine changes during the reaction as a consequence of the isotope effect. [c] Intrinsic isotope effects are corrected for the forward commitment as described in the text. [d] The numbers in parentheses are the number of experimental kinetic isotope effect measurements made for each isotope effect. [e] The kinetic isotope effects which use [5′-^{3}H]inosine or [4′-^{3}H]inosine as the remote label are corrected for the 5′-^{3}H or 4′-^{3}H effect according to the equation (actual KIE) = (observed KIE)([5′- or 4′-^{3}H]inosine KIE).

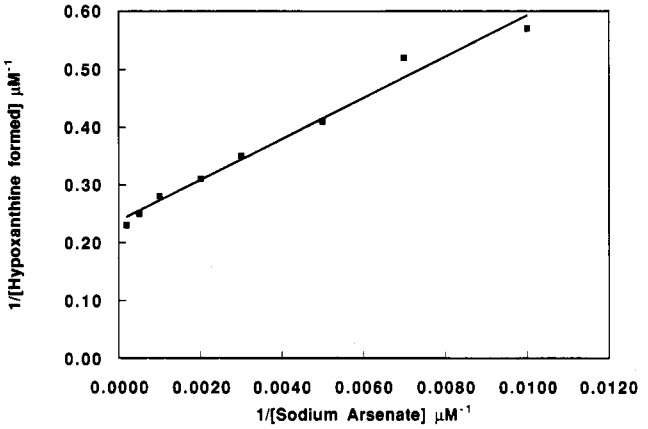

FIGURE 1: Isotope trapping of the PNP·inosine complex by the pulse–chase method. The pulse portion of the experiment contained 400 μM [8-^{14}C]inosine and 30 μM PNP in 50 mM triethanolamine, pH 7.5. The chase solution contained 5 mM inosine, and concentrations of sodium arsenate varied from 0.1 to 10 mM in 50 mM triethanolamine, pH 7.5. The line is drawn from a linear regression of the data. The intercept value indicates that 4.8 μM of [8-^{14}C]-hypoxanthine is formed from 30 μM PNP·[8-^{14}C]inosine complex.

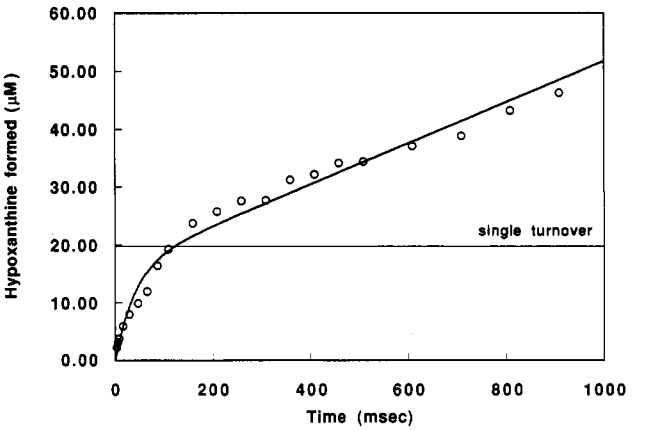

FIGURE 2: Time course of inosine arsenolysis by purine nucleoside phosphorylase. A solution of PNP was mixed with a solution of [8-^{14}C]-inosine, unlabeled inosine, and sodium arsenate to give final concentrations of 400 μM inosine, 25 mM sodium arsenate, and 20 μM PNP in 50 mM triethanolamine, pH 7.5. The product hypoxanthine was isolated by HPLC and quantitated by scintillation counting. The solid line is the best fit to the data points using the kinetic and rate constants shown in Scheme I. The data was fit using the KINSIM program (Barshop et al., 1983). The line labeled "single turnover" is the concentration of PNP subunits (catalytic sites).

Rapid Reaction Kinetics. The unusually small 9-^{15}N kinetic isotope effect for the leaving base, together with the substantial 1′-^{14}C, 1′-^{3}H, and 2′-^{3}H kinetic isotope effects in the ribose ring, suggest that multiple steps may be contributing to the observed isotope effects. The pre-steady-state time course of the reaction was investigated by mixing a solution of purine nucleoside phosphorylase with a reaction mixture containing [8-^{14}C]inosine and sodium arsenate. At various times after mixing, the reaction was quenched by the addition of HCl, and the amounts of radiolabeled inosine and hypoxanthine were determined by HPLC as described in Experimental Procedures. The time-dependent formation of radiolabeled hypoxanthine is shown in Figure 2. A pre-steady-state burst with an amplitude of 1 per enzyme active site is apparent during the first 100 ms, which is followed by a slower, steady-state rate of product formation.

The time course of the reaction was simulated with the KINSIM program using the binding constants for inosine and hypoxanthine determined previously (Kline & Schramm, 1992). The rate of 20 s^{-1} in the initial burst phase of the reaction was approximately 10 times faster than the steady-state rate of 2.0 s^{-1} for arsenolysis at 20 °C. The steady-state rate of phosphorolysis at conditions near V_{max} and at 25 °C is 13 s^{-1} using low concentrations of the calf spleen enzyme (Porter, 1992).

Hydrolysis of Ribose 1-Arsenate. The arsenolysis reaction of PNP was initiated in ^{18}O-labeled water to determine the site of nucleophilic attack during the hydrolysis of ribose 1-arsenate. A similar approach has been reported using P^{18}O$_4$ and NMR analysis for the phosphorolysis reaction. In this case, hydrolysis of ribose 1-phosphate occurs with C–O cleavage (Jordon et al., 1979). However, alkyl esters of arsenates such as glucose 6-arsenate hydrolyze by attack of H_2O on the arsenate due to the strong electrophilic character of arsenate (Ford & Edwards, 1969; Baer et al., 1981). Hydrolysis of ribose 1-arsenate could also occur prior to release from the catalytic site. Since the enzyme stabilizes an oxycarbonium-like transition state, hydrolysis at the catalytic site might favor C–O bond cleavage. If hydrolysis occurs following ribose 1- arsenate release, O–As bond loss would be favored. Arsenolysis of inosine in $H_2{}^{18}O$ will label arsenate if attack is at the arsenic atom and will label ribose if attack is at C1 of ribose 1-arsenate. The ribose formed in the reaction was reduced to ribitol, peracetylated, and subjected to mass spectral analysis. The products of arsenolysis reactions from unlabeled water and from $H_2{}^{18}O$ were compared to the mass spectra of known peracetylated [1-^{18}O]ribitol. The mass spectrum of the labeled control shows the [M + 1] peak at 365 and fragment peaks at 303 and 305 which represent loss of the labeled acetate group and one of the unlabeled acetate groups, respectively. The mass spectra from the reaction mixtures show no incorporation of solvent ^{18}O into the ribose product. The [M + 1] peak occurs at 363, and the main fragment peak occurs at 303, representing loss of an acetate group. Thus, hydrolysis of ribose 1-arsenate proceeds by H_2O attack on the arsenic, resulting in O–As bond loss.

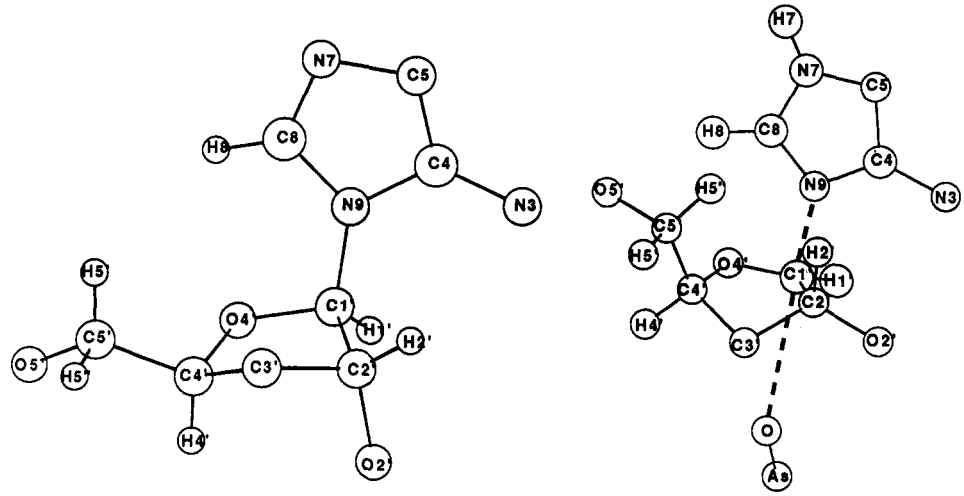

Bond	Ground State	Transition State
C1'-N9	1.47 Å	1.77 ± 0.04 Å
C1'-O4'	1.42 Å	1.29 ± 0.02 Å
C1'-H1'	1.13 Å	1.12 ± 0.01 Å
C1'-C2'	1.53 Å	1.50 ± 0.02 Å
C2'-H2'	1.12 Å	1.16 ± 0.01 Å
C1'-OAs		3.01 ± 0.02 Å
C8-N9	1.37 Å	1.32 ± 0.02 Å
C4-N9	1.37 Å	1.33 ± 0.02 Å
C8-N7	1.31 Å	1.31 ± 0.02 Å

FIGURE 3: The geometry of inosine (left) and inosine at the transition state of the purine nucleoside phosphorylase reaction (right). Only the atoms used in the bond energy–bond order vibrational analysis are shown. Bond lengths are given in Å. Note the protonation of N7, the lengthened C1′–N9 bond, the shortened C1′–O4′ bond, the rehybridization of C1′ to near-sp^2 geometry, the 3′-*exo* configuration of the ribose ring, the eclipsed H2′–C2′ and C1′–N9 bonds at the transition state, and the attacking oxygen of the arsenate anion. Not obvious from the figure is the geometric strain at C5′ which causes the 5′-^{3}H isotope effect.

Transition-State Modeling. The kinetic isotope effects obtained for the arsenolysis reaction were matched to a vibrational transition state using bond energy–bond order vibrational analysis (Sims & Lewis, 1984). An acceptable transition state was one in which the experimentally observed isotope effects were matched to the kinetic isotope effects calculated for a specific model of transition-state vibrational structure and geometry. The procedure to select the appropriate transition state was based on the transition-state determinations for AMP nucleosidase and nucleoside hydrolase (Horenstein et al., 1991; Parkin et al., 1991). In these transition states, substantial oxycarbonium ion character has been developed between C1′ and O4′, extensive hyperconjugation exists between the C2′–H2′ and C1′–N9 bonds, and a low bond order exists between the anomeric carbon and the incoming nucleophile (see Figure 3 for atomic labels).

The range of acceptable transition states is defined in part by the requirement for strong hyperconjugation between C2′–H2′ and C1′–N9 for substantial 2′-^{3}H isotope effects (Mentch et al., 1987). This limits the conformations that can be present in the transition state to ones in which the dihedral angle between the C2′–H2′ and C1′–N9 bonds is eclipsed or near to eclipse. Under these conditions, the 2′-^{3}H isotope effect is a near-linear function of C2′–H2′ bond order. A bond order of 0.82 was found to agree most closely with the substantial 2′-^{3}H secondary kinetic isotope effect of 1.152 ± 0.003. Another variable in the transition state was the bond order between C1′ and H1′, which must match the 1′-^{3}H isotope effect of 1.141 ± 0.004. *Ab initio* calculations indicate that this bond should become slightly shorter as the oxycarbonium ion character increases.[1] The transition state which matches the intrinsic kinetic isotope effects has a C1′–H1′ bond order of 0.93 compared to that of 0.90 in the reactant inosine. The normal isotope effect at H1′ arises primarily from the increased freedom in the out-of-plane bending mode for H1′ at the transition state.

The small ^{15}N intrinsic kinetic isotope effect of 1.010 ± 0.005 is a key experimental result for the determination of the transition-state structure. Because of its low value, the bond order to N9 must remain relatively high at the transition state. Protonation of N7 in the hypoxanthine ring causes a change in the bond orders between N7–C8 and C8–N9. While the total bond order is conserved in the imidazole ring, there is an increase in the bond order between C8 and N9 and a decrease in the bond order between C8 and N7. The ratio of N7–C8/N9–C8 bond orders changes from 1.27 to 0.86 upon protonation of N7. This change is consistent with the observed increase in bond order around N9 within the purine ring to account for the low ^{15}N kinetic isotope effect. The other bond order which influences the 9-^{15}N isotope effect is the bond order between C1′ and N9. A bond order of 0.4 for this bond produced the appropriate kinetic isotope effect while maintaining the C4–N9 and C8–N9 bond orders at chemically reasonable values. With the C1′–N9 bond order at 0.4, the C8–N9 and C4–N9 bond orders were 1.72 and 1.70, respectively. The total bond order to N9 was 3.82 at the transition state compared to 4.03 in the ground state. The C8–N9 bond order is consistent with the changes known to occur as a result of N7 protonation. However, the increase

[1] Dr. B. A. Horenstein, communication based on Gaussian 92 molecular orbital calculations of model compounds.

in C4–N9 bond order indicates that the hypoxanthine ring experiences some distortion in the transition state, consistent with the observation that hypoxanthine is tightly bound by the enzyme (Kline & Schramm, 1992).

It was necessary to include a low bond order to the attacking nucleophile to account for the 1′-^{3}H isotope effect. However, the attacking arsenate oxygen is positioned at the relatively long distance of 3 Å. The loss of most of the C1′–N9 bond order without substantial bond formation to the arsenate causes the C1′–O4′ bond to be considerably shortened in the transition state to 1.29 ± 0.02 Å. This feature indicates considerable oxycarbonium ion character at the transition state.

The transition state which matches the experimental isotope effects is shown in Figure 3. The standard errors associated with the bond lengths in Figure 3 were determined by varying the bond orders adjacent to the glycosidic bond until at least one of the predicted isotope effects was outside the error range of the experimental isotope effects.

The transition state for purine nucleoside phosphorylase contains substantial oxycarbonium ion character, while there is very little bond order between C1′ and the attacking arsenate oxygen. Protonation has occurred at N7 to assist departure of the hypoxanthine. Loss of the C1′–N9 bond is not as advanced as with the *N*-glycohydrolase reactions (Parkin et al., 1991; Horenstein et al., 1991); however, additional distortion occurs within the purine base to maintain a high bond order around N9.

DISCUSSION

Kinetic Mechanism for PNP. Kinetic mechanisms have been proposed for purine nucleoside phosphorylases from a variety of sources (Kim et al., 1968; Krenitsky, 1967; Parks & Agarwal, 1972; Lewis, 1977; Barsacchi et al., 1992; Porter 1992). In all cases a covalently bound enzyme intermediate was deemed to be inconsistent with the data. For the human enzyme Kim et al. (1968) concluded that the mechanism is ordered bi bi with inosine binding first and ribose 1-phosphate being released first. Similar results have been reported for the calf spleen enzyme (Krenitsky, 1967). Recently Porter (1992) has reported from fluorescence measurements that phosphate binds before the nucleoside. However, a strictly ordered mechanism is inconsistent with the substantial 1′-^{3}H and 2′-^{3}H kinetic isotope effects found for the arsenolysis reaction. Nucleoside binding first in an ordered mechanism would cause the kinetic isotope effect for inosine to approach unity when arsenate (or phosphate) is saturating, since saturation with a second substrate prevents release of the first, increases the commitment factor, and abolishes the kinetic isotope effects. A requirement for arsenate (or phosphate) to bind first would also prevent the trapping of inosine which clearly occurs with the calf spleen enzyme. These results require the binding of substrates to be random.

Chemical Mechanism of Arsenolysis. The low ^{15}N kinetic isotope effect suggested the possibility that arsenolysis occurs in two distinct chemical steps, the first being formation of ribose 1-arsenate, followed by hydrolysis of ribose 1-arsenate at the catalytic site of the enzyme rather than in solution. In this mechanism the cleavage of the C–N bond takes place before the first irreversible step so there would be combined equilibrium and kinetic isotope effects for N9. The isotope effects from the isotopic substitutions in ribose would then result from the enzyme-assisted hydrolysis of ribose 1-arsenate. This mechanism was inconsistent with the ^{18}O labeling experiments, which demonstrated that the site of nucleophilic attack during hydrolysis was arsenic rather than carbon.

Scheme I

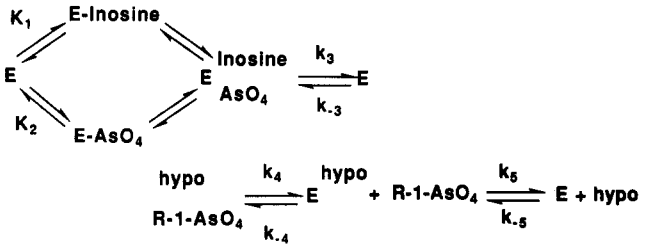

Parameter	
K_1	7.8 μM
K_2	1800 μM
k_3	20 s^{-1}
k_{-3}	0.01 s^{-1}
k_4	200 s^{-1}
k_{-4}	0.001 μM^{-1} s^{-1}
k_5	2 s^{-1}
k_{-5}	1.25 μM^{-1} s^{-1}

Hydrolysis at the arsenic atom would not cause the observed isotope effects with labeled ribose. This eliminates an enzyme-catalyzed hydrolysis of ribose 1-arsenate as a step of the reaction sequence.

A direct S_N2 nucleophilic attack of arsenate at C1′ can also be eliminated by the magnitude of the isotope effects. Nucleophilic displacements result in a relatively large isotope effect from the atom at the reaction center (C1′) but small or absent isotope effects from α- and β-secondary effects (Mentch et al., 1987).

Rapid Reaction and Substrate Trapping Kinetics. The burst of product formation which precedes the steady-state rate of product formation requires a step subsequent to C–N bond cleavage to be rate limiting. Product release of hypoxanthine is the most likely step since hypoxanthine is tightly bound during the hydrolytic reaction of PNP and binds with a dissociation constant of 1.7 μM in the presence of phosphate (Kline & Schramm, 1992; Agarwal & Parks, 1969). The burst in the rapid reaction kinetics would be due to cleavage of the C–N bond followed by the rapid release of ribose 1-arsenate and the steady-state rate of hypoxanthine release. This mechanism is consistent with results for the phosphorolysis of guanosine (Porter, 1992), where the slowest steady-state step is the dissociation of guanine from the enzyme·base complex. For the phosphorolysis reaction, it was reported that phosphate binds first, followed by inosine (Porter, 1992). For the arsenolysis reaction, ordered binding with arsenate first is inconsistent with both the kinetic isotope effects and the substrate-trapping experiment. The presence of significant isotope effects in the presence of near-saturating concentrations of both substrates indicates a random addition of the two substrates. Substrate trapping experiments demonstrate that a commitment factor of 0.19 exists for inosine bound to PNP in the absence of arsenate. Substrate trapping can only occur if a catalytically competent binary complex forms in the absence of arsenate.

Kinetic Mechanism for Purine Nucleoside Phosphorylase. A mechanism is proposed which includes the random addition of substrates followed by cleavage of the C–N bond as the enzyme-catalyzed step which gives rise to the observed isotope effects (Scheme I). The release of ribose 1-arsenate is the kinetically irreversible step due to initial rate conditions and to rapid solution hydrolysis of ribose 1-arsenate. However, the slowest step in the catalytic cycle is release of hypoxanthine. The reaction was modeled using KINSIM, and the kinetic

parameters consistent with both the steady-state and the rapid reaction kinetics are shown in Scheme I. The association constant k_{-5} was calculated from the K_d of 1.7 μM for hypoxanthine and the value of k_5 determined from the steady-state rate of arsenolysis. The value of 1.25 μM^{-1} s^{-1} for k_{-5} compares favorably to that of 1.5 ± 0.4 μM^{-1} s^{-1} found for phosphorolysis (Porter, 1992). However, the pre-steady-state burst and the entry to the steady-state rate are relatively insensitive to the k_{-5} rate for hypoxanthine. The results require that the dissociation rate for ribose 1-arsenate be fast (>200 s^{-1}) compared to other steps. This is also consistent with the findings of Porter for phosphorolysis where the k_{off} for ribose 1-phosphate was estimated to be >500 s^{-1} (Porter, 1992).

Kinetic Isotope Effects and Transition-State Structure. The presence of a significant commitment to catalysis for inosine results in the suppression of the intrinsic kinetic isotope effects. To measure the commitment to catalysis for the arsenolysis reaction, isotope trapping with inosine demonstrated that 16% of the bound substrate was converted to product when arsenate was added at saturating concentrations. Reverse commitments do not occur in arsenolysis due to the rapid and irreversible release of this product under initial rate conditions and the accompanying rapid hydrolysis of ribose 1-arsenate. Kinetic isotope effect studies of the phosphorolysis of inosine suffer from the reversible nature of the reaction which favors nucleoside formation. Thus, suppression of isotope effects is likely to occur by both forward and reverse commitments during phosphorolysis, causing negligible observed isotope effects (Table I).

The observed isotope effects for the arsenolysis reaction are corrected for the commitment by using the equation derived by Northrop (1981) to provide intrinsic isotope effects. The magnitude of the 1′-^{3}H and 2′-^{3}H isotope effects establishes the oxycarbonium ion character of the transition state. The large 2′-^{3}H effect demonstrates hyperconjugation to C2′. This fixes the geometry of the 2′-OH group at the transition state, since the isotope effect is a maximum when the dihedral angle between H2′–C2′ and the leaving group bond to C1′ is near 0°. A dihedral of ~180° would result in a similar effect but is ruled out from steric configurations. This isotope effect reduces to near unity at dihedral angles near 90° (Sunko et al., 1977).

The transition state is relatively early with substantial bond order of 0.4 between C1′ and N9 and very little bond order from the attacking nucleophile. By contrast, the C1′–N9 bond orders at the transition state are near 0.1 for acid-catalyzed solvolysis of AMP and approximately 0.2 for the transition state of AMP nucleosidase (Mentch et al., 1987). The nonspecific nucleoside hydrolase from *Crithidia fasciculata* has a C1′–N9 bond order of 0.27 at the transition state (Horenstein et al., 1991). Thus, the transition state of PNP occurs early in the reaction coordinate, with little bond formation to the attacking anion.

The isotope effect from the 5′-^{3}H indicates a change in the geometry at the 5′-C at the transition state. The normal isotope effect indicates a loosening of this bond in the transition state. Other studies have also implicated the role of this group in stabilizing (or reaching) the transition state. For example, Jordan and Wu (1978) indicated that the 5′-methyl nucleosides bind to the enzyme but are not substrates. The crystal structure for PNP shows His257 positioned to hydrogen bond to the hydroxylic hydrogen, and this could provide sufficient distortion force to cause the observed isotope effect. Anchoring of the transition state by enzymic interactions with groups remote from the site of chemical attack is clearly an important feature of enzymic catalysis (Kati, 1992). The remote δ-^{3}H isotope effect of 1.051 in the nucleoside hydrolase reaction provides another example of this effect (Horenstein et al., 1991).

Correlation with Protein Structure. The crystal structure for human erythrocyte PNP in which 9-deazainosine and sulfate anion have been bound in the active site can be used as a guide for the calf spleen enzyme since the homology of the calf spleen enzyme with the human enzyme is 87% overall and 100% within the active site.[2] However, an examination of the crystal structure offers few clues relevant to the chemistry employed by the enzyme. There are no obvious groups near the bound ligand that could stabilize the oxycarbonium ion and none which suggest formation of a covalent intermediate. However, the nearest oxygen of the bound sulfate, which is presumably bound at the phosphate site, is 4.2 Å away from the C1′ of the ribosyl group. These distances are consistent with a dissociative mechanism in which the C1′ region of the ribosyl group is translated from the purine base toward the reacting anion. The 5′-OH and neighboring groups of the ribosyl could function as a hinge for this motion. The extraordinary tight binding (1.3×10^{-12} M) observed for hypoxanthine in the hydrolytic reaction of PNP (Kline & Schramm, 1992) and the unusually high glycosidic bond order at the transition state suggest that enzymatic contacts in the purine are also important in initiating ribosyl expulsion. Since there are few contacts apparent from the crystal structure which could initiate these changes, it is likely that substantial changes will be found in enzyme configuration when structures are available for PNP bound to transition-state analogues.

CONCLUSIONS

Arsenolysis of inosine by purine nucleoside phosphorylase involves random binding of substrates,with a fraction of the bound inosine being committed for catalysis. Product release is characterized by the rapid release of ribose 1-arsenate followed by the rate-limiting release of hypoxanthine. The transition state has considerable oxycarbonium ion character with only weak involvement of the attacking arsenate. The transition state is earlier (greater C1′–N9 bond order) than for the N-glycohydrolases. There is evidence for strong interactions from the enzyme through the hypoxanthine ring and the 5′-region of the ribosyl ring which lead to transition-state distortions of both groups. One enzymatic group responsible for these distortions is His257, which interacts with the 5′-hydroxymethyl of inosine, but few groups can be identified which stabilize the proposed oxycarbonium ion transition state. A mechanism consistent with the results has the purine ring and the C5′–OH group of inosine firmly anchored at the transition state with reaction coordinate motion involving the translocation of C1′ from N9 toward the bound anion nucleophile.

ACKNOWLEDGMENT

The authors thank Dr. Steven Ealick, Cornell University, for providing coordinates for the crystal structure of PNP and Dr. Steven Almo, Albert Einstein College of Medicine, for help with molecular modeling of the PNP structure. We thank Dr. David Parkin for early work on this project, including the data of Table I. Mass spectral analyses were performed in the Laboratory for Macromolecular Analysis, Albert Einstein

[2] Coordinates and sequence information kindly provided by Dr. Steven Ealick, Cornell University.

College of Medicine. The authors thank Mr. Edward Nieves for his help with mass spectrometry.

REFERENCES

Agarwal, R. P.,& Parks, R. E., Jr. (1969) *J. Biol. Chem. 244*, 644–647.

Baer, C. D., Edwards, J. O., & Rieger, P. H. (1981) *Inorg. Chem. 20*, 905–907.

Barsacchi, D., Cappiello, M., Tozzi, M. G., Corso, A. D., Peccator, M., Camici, M., Ipata, P. L., & Mura, U. (1992) *Biochim. Biophys. Acta 1160*, 163–170.

Barshop, B. A., Wrenn, R. F., & Frieden, C. (1983) *Anal. Biochem. 130*, 134–145.

Blakeney, A. B., Harris, P. J., Henry, R. J., & Stone, B. A. (1983) *Carbohydr. Res. 113*, 291–299.

Cleland, W. W. (1987) *Bioorg. Chem. 15*, 282–302.

Cortes, S., Mega, T. L., & Van Etten, R. L. (1991) *J. Org. Chem. 56*, 943–947.

Ealick, S. E., Rule, S. A., Carter, D. C., Greenhough, T. J., Babu, Y. S., Cook. W. J., Habash, J., Helliwell, J. R., Stoeckler, J. D., Parks, R. E., Jr., Chen, S., & Bugg, C. E. (1990) *J. Biol. Chem. 265*, 1812–1820.

Edwards, Y. H., Edwards, P. A., & Hopkinson, D. A. (1973) *FEBS Lett. 32*, 235–237.

Ford, G. C., & Edwards, I. (1969) *Int. J. Mass Spectrom. Ion Phys. 2*, 95–97.

Gelfand, E. W., Dosch, H. M., & Bigger, W. D. (1978) *J. Clin. Invest. 61*, 1071–1080.

Giblett, E. R., Ammann, A. J., Wara, D. W., Sandman, R., & Diamond, L. K. (1975) *Lancet 1*, 1010–1013.

Horenstein, B. A., & Schramm, V. L. (1993a) *Biochemistry 32*, 7089–7097.

Horenstein, B. A., & Schramm, V. L. (1993b) *Biochemistry 32*, 9917–9925.

Horenstein, B. A., Parkin, D. W., Estupiñán, B., & Schramm, V. L. (1991) *Biochemistry 30*, 10788–10795.

Jordan, F., & Wu, A. (1978) *J. Med. Chem. 21*, 877–882.

Jordan, F., Patrick, J. A., & Salamone, S., Jr. (1979) *J. Biol. Chem. 254*, 2384–2386.

Kati, W. M., Acheson, S. A., & Wolfenden, R. (1992) *Biochemistry 31*, 7356–7366.

Kazmers, I. S., Mitchell, B. S., Dadonna, P. E., Wetring, L. L., Townsend, L. B., & Kelley, W. N. (1981) *Science 214*, 1137–1139.

Kim, B. Y., Cha, S., & Parks, R. E., Jr. (1968) *J. Biol. Chem. 243*, 1771–1776.

Kinoshita, Y., Ruble, J. R., & Jeffrey, G. A. (1981) *Carbohydr. Res. 92*, 1–7.

Kline, P. C., & Schramm, V. L. (1992) *Biochemistry 31*, 5964–5973.

Kouba, R. F., & Varner, J. E. (1959) *Biochem. Biophys. Res. Commun. 1*, 129–132.

Krenitsky, T. (1967) *Mol. Pharmacol. 3*, 526–536.

Lehikoinen, P. K., Sinnott, M. L., & Krenitsky, T. A. (1989) *Biochem. J. 257*, 355–359.

Lewis, A. S. (1977) *J. Biol. Chem. 252*, 732–738.

Markham, G. D., Parkin, D. W., Mentch, F., & Schramm, V. L. (1987) *J. Biol. Chem. 262*, 5609–5615.

Mentch, F., Parkin, D. W., & Schramm, V. L. (1987) *Biochemistry 26*, 921–930.

Merz, K. M., Jr., & Besler, B. H. (1990) *Quantum Chemistry Program Exchange*, No. 589, Indiana University, Bloomington, IN.

Munns, A. R. I., & Tollin, P. (1970) *Acta Crystallogr., Sect. B 26*, 1101–1113.

Northrop, D. B. (1981) *Annu. Rev. Biochem. 50*,103–131.

Parkin, D. W., & Schramm, V. L. (1984) *J. Biol. Chem. 259*, 9418–9425.

Parkin, D. W., & Schramm, V. L. (1987) *Biochemistry 26*, 913–920.

Parkin, D. W., Leung, H. B., & Schramm, V. L. (1984) *J. Biol. Chem. 259*, 9411–9417.

Parkin, D. W., Mentch, F., Banks, G. A., Horenstein, B. A., & Schramm, V. L. (1991) *Biochemistry 30*, 4586–4594.

Parks, R. E., Jr., & Agarwal, R. P. (1972) in *The Enzymes* (Boyer, P. D., Ed.) Vol. 7, pp 483–514, Academic Press, New York.

Porter, D. J. T. (1992) *J. Biol. Chem. 267*, 7342–7351.

Rose, I. A. (1980) *Methods Enzymol. 64*, 47–83.

Siegenbeek, L. H., Akkerman, J. W., & Staal, J. E. G. (1977) *Clin. Chim. Acta 74*, 271–279.

Sims, L. B., & Fry, A. (1974) Special Publication No. 1, University of Arkansas, Fayetteville, AR.

Sims, L. B., & Lewis, D. E. (1984) in *Isotopes in Organic Chemistry* (Buncel, E., & Lee, C. C., Eds.) Vol. 6, pp 161–259, Elsevier, New York.

Sims, L. B., Burton, G. W., & Lewis, D. E. (1977) *Quantum Chemistry Program Exchange*, No. 337, Indiana University, Bloomington, IN.

Stein, R. L., & Cordes, E. H. (1981) *J. Biol. Chem. 256*, 767–772.

Stewart, J. J. P. (1989) *Comput. Chem. 10*, 209–220.

Stoeckler, J. D., Ealick, S. E., Bugg, C. E., & Parks, R. E., Jr. (1986) *Fed. Proc. 45*, 2773–2778.

Sunko, D. E., Szele, I., & Hehre, W. J. (1977) *J. Am. Chem. Soc. 99*, 5000–5005.